JOURNAL OF AGRICULTURAL AND FOOD CHEMISTRY

Article

pubs.acs.org/JAFC

Polyphosphates and Fulvates Enhance Environmental Stability of PO_4-Bearing Colloidal Iron Oxyhydroxides

Jessica Bollyn,[*,†] Mathias Nijsen,[†] Stijn Baken,[†,#] Iris Joye,[‡] Nadia Waegeneers,[§] Geert Cornelis,[∥] and Erik Smolders[†]

[†]Department of Earth and Environmental Sciences, KU Leuven, Kasteelpark Arenberg 20 bus 2459, 3001 Leuven, Belgium

[‡]Department of Microbial and Molecular Systems, KU Leuven, Kasteelpark Arenberg 22 bus 2463, 3001 Leuven, Belgium

[§]Service Trace Elements, CODA-CERVA, Leuvensesteenweg 17, 3080 Tervuren, Belgium

[∥]Department of Soil and Environment, SLU, Box 7014, 750 07 Uppsala, Sweden

Supporting Information

ABSTRACT: Iron oxyhydroxide nanoparticles (Fe-NPs) are natural vectors of phosphate (PO_4) in the environment. Their mobility is determined by colloidal stability, which is affected by surface composition. This might be manipulated in engineered NPs for environmental or agricultural applications. Here, the stability of PO_4-Fe-NPs (HFO/goethite) was determined across contrasting environmental conditions (pH, Ca concentration) and by using fulvates (FA) and polyphosphates (poly-P's) as coatings. The PO_4-Fe-NPs are unstable at Ca concentrations above 0.1 mM. Addition of FA and some poly-P's significantly improved stability. Zeta potential explained colloidal stability across treatments; surface charge was calculated with surface complexation models and explained for phytic acid (PA) and hexametaphosphate (HMP) by a partial (1−4 of the 6 PO_4 units) adsorption to the surface, while the remaining PO_4 units stayed in solution. This study suggests that Ca concentration mainly affects the mobility of natural or engineered PO_4-Fe-NPs and that HMP is a promising agent for increasing colloidal stability.

KEYWORDS: *iron oxyhydroxide nanoparticles, colloidal stability, phosphate transport, polyphosphate, natural organic matter, phytate*

INTRODUCTION

Naturally occurring colloids are defined as particles smaller than 1 μm, while nanoparticles (NPs) are defined as particles having at least one dimension between 1 and 100 nm. Naturally occurring NPs play an important role in the environment as carriers of compounds that adsorb strongly to their surface. This surface complexation enhances their mobility, since several of these compounds would otherwise demonstrate little transport in most natural waters or soils. Iron oxyhydroxide NPs (Fe-NPs), in particular, often act as efficient carriers for phosphate (PO_4),[1−4] metals,[5] and natural organic matter (NOM),[6] because they strongly bind these compounds, have a large surface area, and sometimes have high mobility.[7]

Particle-mediated transport is rarely taken into account in most solute transport models, which rely on thermodynamic approaches that cannot accurately describe the fate of particles in the environment.[8] Many studies have investigated the structure and mineralogy of the Fe-NPs, whereas knowledge on factors affecting Fe-NP transport is scarce.[9−12] A high colloidal stability, implying a low rate of aggregation, under environmental conditions is crucial to particle mobility. Particle aggregation leads to poor mobility in most soils, because the aggregates can no longer access the smallest of pores.[13] In addition, the same factors leading to poor colloidal stability often cause faster attachment of colloids to pore walls.[13]

In aquatic systems, formation of natural Fe-NPs occurs at the oxic−anoxic boundary, e.g., when groundwater surfaces, where Fe(II) oxidation leads to formation of colloidal hydrous ferric oxide (HFO), which can subsequently transform to other iron oxyhydroxide minerals, i.e., goethite.[14] The rates of these processes are highly dependent on different factors, ultimately also determining colloidal stability of the resulting Fe-NPs, since different phase formations will likely lead to differences in colloidal stability.[15] A recent study indicated that humic acid (HA) inhibits transformation of ferrihydrite into goethite and lepidocrocite.[16] Also, dissolved silica can control the mineralogy of the formed Fe-NPs: it favors 2-line ferrihydrite formation but also leads to increased PO_4 sorption.[9,17] In other words, PO_4 transport in aquatic systems is controlled by different factors controlling Fe-NP mineralogy and morphology, but these factors could also influence colloidal stability, which has been hardly addressed.[12,15,17]

The colloidal stability of Fe-NPs is enhanced by adsorption of NOM, as has been demonstrated in aquatic and soil systems.[18−20] Adsorption of NOM adds a negative charge on the Fe-NP surface, causing both electrostatic destabilization and electrostatic/steric stabilization, depending on the NOM:NP ratio and solution pH.[21] Conversely, bridging by divalent cations, e.g., calcium, has been reported to aggregate NOM-stabilized systems.[21,22] However, natural Fe-NPs are often coated with PO_4; thus, they also bear a (partially) negative charge. The impact of this on colloidal stability has yet to be investigated.

Recently, particle-mediated transport has received renewed interest in the context of risk assessment and environmental application of engineered NPs in soils.[23,24] Specifically, Fe-NPs

Received: May 30, 2016
Revised: September 8, 2016
Accepted: October 18, 2016
Published: October 18, 2016

DOI: 10.1021/acs.jafc.6b02425
J. Agric. Food Chem. XXXX, XXX, XXX−XXX

have gained increasing attention as environmental nanovectors in soils, for example, as a means for contaminant removal in groundwater aquifers.[25] Other applications might include high-efficiency nanofertilizers for strongly PO_4-fixing soils.[2,26] Since phosphorus is a limited natural resource, the demand for specialized fertilizers, e.g., slow-[27] or controlled-release fertilizers,[28,29] is rapidly growing. Food productivity must increase because of a growing world population and a dwindling surface area of arable land. One way to achieve this could be to mimic and enhance the natural role of Fe-NPs by introducing artificial Fe-NPs with adsorbed PO_4 (PO_4-Fe-NPs) in P-fixing soils. Addition of P to soils releases large amounts of PO_4-Fe-NPs,[4] suggesting a relatively high mobility of these particles that can potentially deliver PO_4 more efficiently to a plant's rhizosphere compared to, e.g., dissolved P fertilizers. Even though PO_4 is strongly adsorbed to Fe-NPs, it could be released again in the rhizosphere. To achieve this, it is necessary to increase the understanding of the colloidal stability of naturally occurring PO_4-Fe-NPs and investigate how colloidal stability can be increased. High colloidal mobility might also lead to increased P runoff via surface water or groundwater, although this effect is probably negligible due to the thermodynamic instability of colloids, leading to settling over longer distances.

The general objective of this study was to assess the colloidal stability of PO_4-Fe-NPs as affected by the surface and solution composition. In addition, this study investigated natural additives to enhance the colloidal stability of engineered PO_4-Fe-NPs in view of the potential application as P-nanofertilizer. This second step was necessary since preliminary experiments showed that Fe-NPs with solely PO_4 adsorbed were not stable under relevant environmental conditions (Supporting Information (SI), Table S1).

In the first part of this study, Fe(II) was oxidized in the presence of PO_4 and NOM, which leads to the formation of hydrous ferric oxide (HFO), mimicking natural Fe-NP formation at redox boundaries. The colloidal stability and zeta potential of the resulting suspensions were measured under varying pH and Ca concentrations, with or without dissolved silica present during formation, since Si is known to affect mineralogy, which is in turn expected to alter PO_4 sorption. In the second part, natural additives, e.g., NOM, were tested as stabilizing coatings for engineered nano-goethite suspensions coated with PO_4 (PO_4-nG). Suspensions were then subjected to several (de)stabilizing combinations of Ca and pH. We speculate that electrostatic interactions dominate the fate of Fe-NPs and coatings that enhance the negative surface charge will improve colloidal stability.

MATERIALS AND METHODS

Chemicals. All chemicals were analytical reagent grade from Fischer Scientific, Acros Organics, Fluka, or Sigma-Aldrich, and all stock solutions were prepared by dilution in analytical reagent water (18.2 MΩ cm^{-1}, Milli-Q purification system, Millipore). Suwannee River NOM (SRNOM, International Humic Substances Society, 2R101N) was used as a model compound for NOM. A NOM stock solution of 1.00 g/L was prepared by dissolving SRNOM in ultrapure water, adjusting it to pH 6.0 with NaOH, and filtering over a 0.45 μm membrane filter (Chromafil Xtra PET 45/25, 25 mm diameter, polyester membrane). The resulting solution was stored in darkness at 4 °C. All glassware was acid-washed overnight in ±0.1 M HCl.

Iron Oxyhydroxide Colloids Formed by Fe(II) Oxidation. Iron oxyhydroxide colloids were synthesized in the presence of dissolved phosphate and NOM using a molar PO_4:Fe ratio of 0.11, a ratio that allows for complete P removal from solution,[11] and a NOM:Fe ratio of 1 mg C/mg Fe. These ratios are commonly encountered in groundwater and ditch water in the Flanders region.[14,30] Total concentrations are on the upper end of measured concentrations in groundwater, but they were chosen to enable a sufficient particle concentration to allow Z-average hydrodynamic diameter (d_h) and electrophoretic mobility measurements of different size fractions. In a 100 mL flask, a background solution of 100 μM $H_2PO_4^-$ (as KH_2PO_4), 100 mg SRNOM L^{-1}, and 50 mM $NaHCO_3$ as a buffer was prepared at pH 7.0 ± 0.1, because most natural waters have a near-neutral pH. Waterglass (Na_2SiO_3) at a final concentration of 450 μM was also added to investigate Fe(II) oxidation in the presence of Si. This concentration was chosen because an initial molar ratio of 0.5 Si/Fe present during Fe(II) oxidation was reported to increase P sorption due to an inhibition to ripen from ferrihydrite to goethite.[9] Finally, a Fe(II) solution ($FeSO_4 \cdot 7H_2O$, 36 mM Fe in 10^{-5} M HCl, freshly prepared) was added at a final concentration of 900 μM Fe to start oxyhydroxide formation, yielding two stock solutions: one in the absence and one in the presence of Si. Samples were shaken to ensure mixing and rested for 24 h to allow near-complete oxidation.[12] The pH remained at pH 7.0 ± 0.1 throughout the synthesis. The total P, Si, and Fe concentrations were determined in an aliquot from the stock solutions after acidification to 1% HNO_3 by inductively coupled plasma mass spectrometry (ICP-MS) measurement (see Analysis).

To determine the size distribution of the formed Fe oxyhydroxide particles, cascade filtration of the two stock solutions was carried out over 1.2 μm (Chromafil Xtra PET 120/25, 25 mm diameter, polyester membrane), 0.45 μm (Chromafil Xtra PET 45/25, 25 mm diameter, polyester membrane), and 0.1 μm (Pall Acrodisc Supor filter, 32 mm diameter, hydrophilic poly(ether sulfone) membrane). The d_h and zeta potential were measured in filtrates within the hour before and after addition of a range of Ca concentrations (as $CaCl_2$; 0.01−0.1−1 mM Ca) to assess stability in the presence of divalent cations (see Analysis for details on d_h and zeta measurements). Additionally, the properties of the particles at different pH values were tested for both stock solutions by addition of HCl or NaOH to a subsample and measurement of d_h and zeta potential at eight different pH values.

Each stock was subjected to dialysis (Spectra/Por 4, 12−14 kDa cutoff, Spectrum Laboratories Inc.) to determine free and particulate, defined as >14 kDa, elemental concentrations. Dialysis membranes were soaked prior to use for at least 24 h and then filled with 2.5 mL of Milli-Q water (Millipore Corp.), closed, and immersed in 10 mL of stock solution. Samples were shaken for 48 h on a rotary shaker to establish equilibrium, and then samples from both external and internal solutions were analyzed with ICP-MS. Concentrations of particulate bound elements were calculated as difference in elemental concentration between external solution and internal solution. It was assumed that the composition of the <12 kDa fraction equals that of the true solution.

Engineered Iron Oxyhydroxide NPs. An engineered commercially available iron(III)-oxide nanoparticulate dispersion (Sigma-Aldrich, 20 wt% in water, pH 3.5−4.0) was used in the second experimental part. The goethite (FeOOH) mineralogy was confirmed using XRD-analysis (SI, Figure S1). Specific surface area was measured with BET-N_2 sorption and potentiometric titration (SI, Section 2). A stock solution of 0.2 wt% was prepared by dilution with analytical reagent water (resistivity of 18.2 MΩ cm^{-1}, Milli-Q purification system, Millipore) for further sample preparation. Hydrodynamic diameter was regularly checked with DLS to assess aggregation over time, no aggregation was measured during the time frame of our experiments. The average d_h at 20 g NP/L was 64.5 nm.

The nano-goethite (nG) was coated with PO_4 and a stabilizing coating by diluting nG stock in Milli-Q water and adding the necessary components, always including PO_4. Preliminary tests were carried out with different components, of which only SRNOM and some polyphosphates (poly-P's) proved to increase colloidal stability of the PO_4-coated nG. The different poly-P's used in this study were sodium tripolyphosphate (TPP), sodium pyrophosphate tetrabasic (PP), trisodium trimetaphosphate (TMP), sodium hexametaphosphate (HMP), and phytic acid sodium salt hydrate (PA), also known as myo-inositol hexakisphosphate. All stock solutions, besides the nG stock, were prepared at pH 6.0 and stored at 4 °C in darkness. Nominal PO_4 concentrations were verified with ICP-MS. All measurements were

DOI: 10.1021/acs.jafc.6b02425
J. Agric. Food Chem. XXXX, XXX, XXX−XXX

carried out at 2.25 mM nG. The effect of stabilizing additives was always tested together with PO_4 in different ratios to assess the necessary amount of additive to ensure colloidal stability. The molar unit of the poly-P refers to the complete molecule, not a PO_4 unit in that molecule. In an additional experiment, poly-P's were also dosed at 0.1 mM P on an equal mol P base; i.e., 0.05 mM PP was dosed to yield 0.10 mM total P, etc. These coating concentrations were always above the surface binding capacity of the nG, in order to ensure full surface coverage and to eliminate the percentage of coverage as a factor influencing colloidal stability.

The effect of Ca was tested at different concentrations ranging from 0.1 mM to 1.0 mM $CaCl_2$. After mixing, samples were shaken for 60 min on a horizontal shaker and then rested for 30 min to allow aggregation to become visually detectable. On the visually non-aggregated samples, determination of d_h and zeta potential was carried out. The most stable combinations were tested for pH stability by adjusting pH after mixing by adding HCl or NaOH before size and zeta potential measurement at two different PO_4/additive ratios.

Analysis. The d_h was measured with dynamic light scattering (DLS) using a Zetasizer NanoZS (ZEN3600, Malvern Instruments), equipped with a HeNe red laser with a wavelength of 633 nm. The instrument was operated in backscattering mode (at a fixed angle of 173° (non-invasive backscattering)) and at a constant temperature of 25 °C. All samples were analyzed in triplicate. The d_h and polydispersity index (PDI) were calculated from autocorrelation functions using cumulant analysis.

Laser Doppler velocimetry in combination with M3-PALS was used to measure electrophoretic mobility with the Zetasizer NanoZS. The same conditions as for DLS were used, but a fixed angle of 12.8° was employed, and the sample was measured in a folded capillary cell (DTS1070, Malvern Instruments). Henry's equation was used to convert electrophoretic mobility to zeta potential.

Elemental composition of NP dispersions was determined using ICP-MS (Agilent 7700x, Agilent Technologies) after acidification of the sample to 1% HNO_3. Analysis of engineered Fe-NPs was preceded by hot acid digestion with 1.5 mL of HCl and 0.5 mL of HNO_3 for at least 2 h at 140 °C (digestion block). X-ray diffraction (XRD) patterns were measured to confirm mineralogy after freeze-drying under vacuum. Patterns were recorded between 5 and 70° 2θ with a scan step width of 0.02° (Philips PW1830 diffractometer, Cu Kα radiation at 45 kV and 30 mA). Background subtraction and peak analysis were performed with DiffracPlus EVA software (Bruker AXS, Germany). Single-particle ICP-MS (spICP-MS) was performed on selected nG samples stabilized with poly-P or NOM to determine the mass equivalent spherical diameter ($d_{spICP-MS}$) and number-based particle size distribution. Extensive background on this technique can be found elsewhere;[31] details on the measurements are found in SI, section 2.3.

Data Analysis. Data analysis was performed with the statistical program JMP Pro 12 (SAS Institute). Statistical significance was tested with the Student t test with $p < 0.05$. Iso-electric point (IEP) was modeled using a nonlinear three-parameter exponential model. Structure analyses were made with Instant JChem 15.12.7.0 (ChemAxon) and Mercury 3.7 (Cambridge Crystallographic Data Center, UK). Chemical equilibrium modeling was performed with Visual Minteq 3.0 (JP Gustafsson, KTH Stockholm); more details in SI.

RESULTS

Iron Oxyhydroxide Colloids Formed by Fe(II) Oxidation. The oxidation of the Fe-NOM-PO_4 solution, mimicking an environmental relevant groundwater, yielded a colloidal suspension with only a small nanoparticulate fraction as analyzed using cascade filtration (Table 1). As expected, only a small amount of Fe remained in the true solution after 24 h reaction time (Table 2). In contrast, Si was only partially incorporated. The presence of Si during NP formation reduced the colloidal size (Table 1). Regardless of Si addition, the largest colloid population was present in the 0.1−0.45 μm size fraction. Each filtrate was also measured using DLS. The 1.2 and 0.45 μm filtered solutions of both Si treatments had a significantly higher d_h than the 0.1 μm filtrate, respectively around 190 nm and around 150 nm. The 0.1 μm filtrate in the absence of Si had a d_h of 57 nm, while the particles in the presence of Si were slightly smaller at 49 nm. The XRD patterns of both colloidal suspensions are shown in Figure 1; most peaks correspond

Table 1. Size Distribution, Hydrodynamic Diameter, and Chemical Composition of Iron Oxyhydroxide Fractions Formed after 24 h Oxidation of a 900 μM Fe(II) Solution in the Presence of NOM and PO_4 and in the Presence or Absence of Si[a]

	Si present				Si absent		
	d_h	P	Fe	Si	d_h	P	Fe
	nm	%	%	%	nm	%	%
>1.2 μm	202	0	0.20	0	190	3.7	2.4
0.45−1.2 μm	195	7.1	7.0	3.6	184	27	29
0.1−0.45 μm	160	68	69	39	144	58	58
<0.1 μm	49	24	24	58	57	12	10

[a]Size distributions calculated as percentage of total elemental concentration present in each fraction. Z-average hydrodynamic diameter (d_h, DLS) is the mean of three replicate measurements.

Table 2. Percentage of Fe, P, and Si in Solution or in Particulate Form after 24 h Oxidation of a 900 μM Fe(II) Solution in the Presence of NOM and PO_4 and in the Presence or Absence of Si[a]

		Si present	Si absent
$(P:Fe)_{init}$	mol/mol	0.11	0.11
$(Si:Fe)_{init}$	mol/mol	0.5	–
Fe_{free}	%	2.0	2.5
P_{free}	%	7.9	8.3
Si_{free}	%	66	–
$(P:Fe)_{part}$	mol/mol	0.10	0.11
$(Si:Fe)_{part}$	mol/mol	0.18	–

[a]The fraction of free elements refers to the truly dissolved elements, i.e., smaller than 12−14 kDa, determined by dialysis. The particulate fraction is calculated from the difference between total and free elemental concentrations.

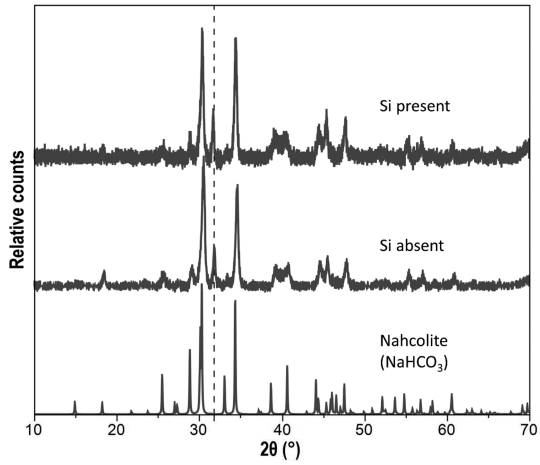

Figure 1. XRD diffractograms of NOM and PO_4-containing iron oxyhydroxide dispersion in the presence or absence of Si. Nahcolite pattern is given as a reference. The vertical dashed line indicates the iron hydroxyphosphate peak. The data have been background corrected and vertically shifted for clarity.

DOI: 10.1021/acs.jafc.6b02425
J. Agric. Food Chem. XXXX, XXX, XXX−XXX

with nahcolite ($NaHCO_3$), which precipitated during freeze-drying. One other peak was identified (dashed line at 31.5°) and attributed to HFO-P, in accordance with Thibault et al.,[32] who found that the first characteristic ferrihydrite peak (35.5° 2θ) becomes more symmetric and shifts to smaller angles with increasing PO_4 concentration present during formation. The presence of Si decreased sharpness of the peaks, pointing to less crystalline or smaller particles,[32] the latter being confirmed by our filtration data.

The dispersion was stable over a pH range from pH 5.0 to 10.0, whereas colloids aggregated (d_h > 1 μm, not quantifiable with DLS) and visually settled within minutes at pH < 5.0, when the zeta potential increased to less negative values (> −30 mV, Figure 2). No difference in zeta potential was found between Fe

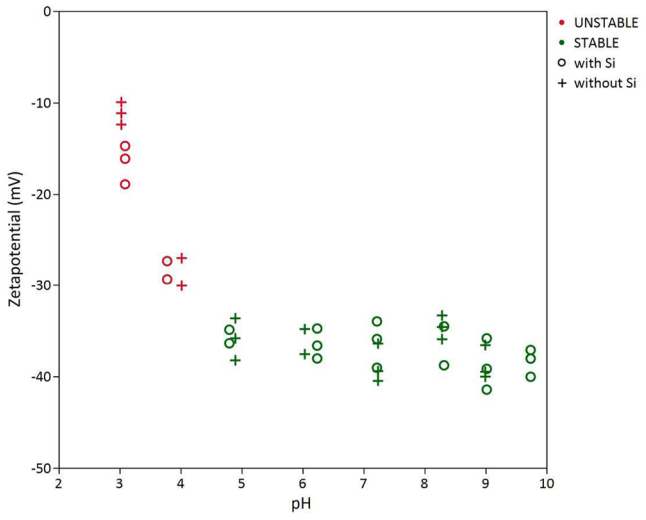

Figure 2. Zeta potential of NOM and PO_4-containing iron oxyhydroxide dispersion, formed in the presence (+) or absence (○) of Si as a function of pH. Green symbols indicate a stable dispersion, red symbols an unstable dispersion defined by a rapidly increasing hydrodynamic diameter as measured by DLS.

oxyhydroxide formed in the presence or absence of Si except at the lowest pH of 3.0, where the Si presence led to a more negative zeta potential. At pH 7.0, increasing the Ca concentration from 0.01 to 1.0 mM Ca reduced colloidal stability, with aggregation visible for all solutions containing 1.0 mM Ca, which was confirmed by d_h measurement (SI, Table S7). This aggregation is associated with a significantly less negative zeta potential at 1.0 mM Ca compared to the low Ca concentration treatment (Table 3), which suggests a significantly lower electrostatic repulsion. No significant difference in aggregation or zeta potential at different Ca concentrations was found between Si treatments.

Engineered Iron Oxyhydroxide NPs. Commercial nG has a strongly positive zeta potential at pH 3.5 (Figure 3), the pH of the stock solution. The IEP for these uncoated nG samples is pH 8.7, a value that corresponds with documented IEP values for natural and synthetic goethite.[33] Around the IEP, the nanoparticulate dispersion was unstable (Figure 3). Several stabilizing agents, i.e., citrate, PVP, poly-P, and NOM, were tested in preliminary tests to assess the colloidal stability with different coatings. Only addition of NOM and poly-P resulted in stable dispersions under the tested pH range combined with increasing Ca concentrations (SI, Table S1).

Both NOM and poly-P add negative charge onto the surface. When only PO_4 was coated onto nG, the IEP shifted to lower

Table 3. Zeta Potential of Iron Oxyhydroxide Fractions Formed after 24 h Oxidation of a 900 μM Fe(II) Solution in the Presence of NOM and PO_4 and in the Presence or Absence of Si[a]

	zeta potential (mV)			
	Si present		Si absent	
Ca (mM)	0.45−1.2 μm	0.1−0.45 μm	0.45−1.2 μm	0.1−0.45 μm
0.01	−35.6	−33.7	−35.7	−33.6
0.1	−34.0	−32.1	−34.3	−34.6
1	−29.5[b]	−32.9	−31.4[c]	−31.5

[a]Size fractions were separated by sequential filtration over 1.2 and 0.45 μm filters; data from size fraction filtered over 0.1 μm filter not shown because the concentration was too low for zeta potential measurement. [b]p-value <0.05 in Student t test compared to low Ca concentration. [c]p-value <0.01 in Student t test compared to low Ca concentration.

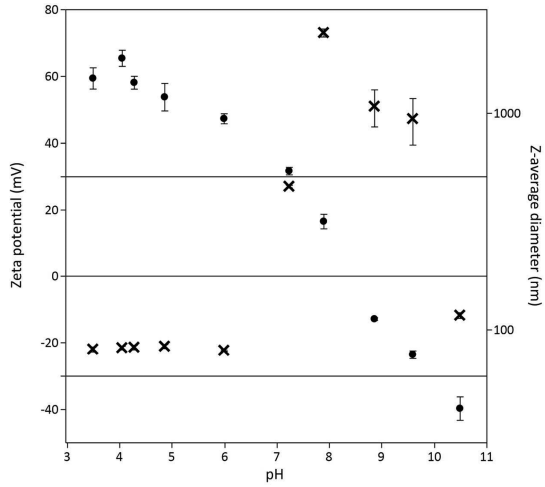

Figure 3. Zeta potential (●) and Z-average diameter (×) of engineered nano-goethite determined with DLS relative to pH of dispersion. Error bars indicate standard deviation of three replicate measurements. Instability zone for electrostatically stabilized systems is indicated between −30 mV and 30 mV zeta potential.

values (Table 4), but at the environmentally relevant pH range in soils, the dispersions were unstable (Table 5). All data used to model the IEPs can be found in the SI (Figures S5 and S6). The additives decreased the IEP drastically; moreover, a much lower concentration of additives was needed compared to PO_4 to decrease the IEP, indicating their value as a stabilizer.

At the highest additive:nG ratio, and in the absence of Ca, almost all combinations showed stability over the whole pH range, indicated by a low or no IEP (Table 4). Polyphosphates exhibited the most negative zeta potentials at the high additive:nG ratio combined with a small size, indicating electrostatically stabilized systems (Table 5). At equal poly-P:nG ratio but increased PO_4 concentration (higher PO_4:nG), zeta potential became less negative, which would indicate competition of PO_4 with the poly-P thereby reducing the stabilizing effect of poly-P. This was not observed for the NOM-stabilized system: no significant difference in zeta potential was measured at different PO_4:nG ratios. Additionally, selected samples were measured with spICP-MS to determine the size distribution (SI, Figures S2 and S3). Addition of NOM, PA, or HMP only enlarged the mean size with a few nm (Table 5). Differences among d_h are much larger since the adjacent electric double layer is also incorporated.

DOI: 10.1021/acs.jafc.6b02425
J. Agric. Food Chem. XXXX, XXX, XXX−XXX

Table 4. Isoelectric Points for 200 mg Nano-goethite (nG) L^{-1} As Affected by Coating with Natural Organic Matter (NOM) or Different Polyphosphates: Phytic Acid (PA), Hexametaphosphate (HMP), or Pyrophosphate (PP)[a]

	additional coating								
	none	NOM		PA		HMP		PP	
		ratio NOM:nG		ratio PA:nG		ratio HMP:nG		ratio PP:nG	
PO_4:nG		0.05	0.25	0.007	0.033	0.003	0.031	0.010	0.049
0.045	5.01	4.67	2.38	n.m.	n.m.	3.47	1.45	n.m.	n.m.
0.45	3.78	3.40	1.10	<0	<0	1.12	<0	2.10	0.33
4.5	3.19	1.76	1.44	<0	<0	1.23	<0	1.48	<0

[a]All ratios are given as molar ratios except NOM:nG, which is given as a mass ratio. IEP was modeled by nonlinear modeling using a 3P-exponential fit on zeta potential data in a pH range from 3 to 11 with three replicates. n.m. indicates not measured, <0 indicates no IEP physically possible (IEP < 0).

Table 5. Hydrodynamic Diameter (d_h), Diameter Measured with Single-Particle Inductively Coupled Plasma Mass Spectrometry (d_{spIPMS}), and Zeta Potential (ζ) at a Concentration of 200 mg Nano-goethite (nG) L^{-1} and Various Combinations of PO_4, Polyphosphates (Phytic Acid, PA; Hexametaphosphate, HMP; and Pyrophosphate, PP), and NOM at pH 6[a]

		Fe-NP	PO_4:nG = 0.45								
				ratio NOM:nG		ratio PA:nG		ratio HMP:nG		ratio PP:nG	
			–	0.05	0.25	0.007	0.033	0.003	0.031	0.010	0.049
d_h	nm	68.0	n.m.	90.1	82.5	148.0	84.1	190.6	86.0	144.4	98.6
ζ	mV	47.2	−38.47	−44.2	−44.9	−49.6	−58.4	−50.3	−54.0	−48.7	−54.6

		Fe-NP	PO_4:nG = 4.5								
				ratio NOM:nG		ratio PA:nG		ratio HMP:nG		ratio PP:nG	
			–	0.05	0.25	0.007	0.033	0.003	0.031	0.010	0.049
d_h	nm	68.0	328.3	91.8	82.3	97.8	78.4	99.8	78.4	140.4	99.2
$d_{spICP-MS}$	nm	42			47		46		46		
ζ	mV	47.2	−44.3	−43.9	−44.3	−44.8	−43.6	−44.1	−49.1	−45.7	−44.0

[a]Values are the mean of three replicates; for $d_{spICP-MS}$ the median of the size distribution is taken per replicate. All ratios are given as molar ratios, except NOM:nG, which is given as a mass ratio. n.m. indicates not measurable, i.e., sample too polydisperse for DLS measurement, indicating aggregation and sedimentation during measurement.

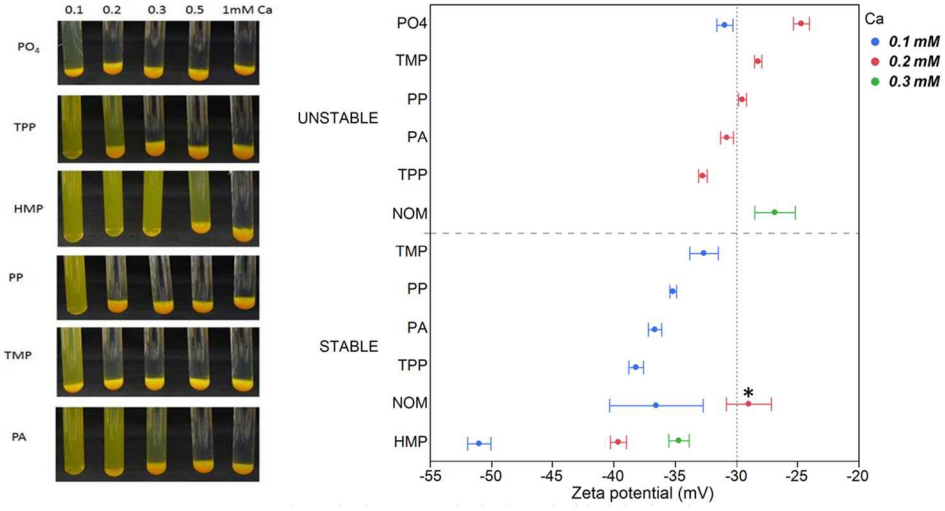

Figure 4. Colloidal stability of 200 mg nano-goethite L^{-1} with 1.0 mM KH_2PO_4, 0.1 mM polyphosphate, and a varying concentration of $CaCl_2$ at pH 6.0. Abbreviations used: TPP , tripolyphosphate; HMP, hexametaphosphate; PP, pyrophosphate; TMP, trimetaphosphate; PA, phytic acid. Left: Samples after 1 h shaking and 30 min resting. Right: Zeta potential of selected samples, measured in triplicate. Error bars indicate standard deviations. NOM is also included as a stabilizing additive at a Fe:NOM mass ratio equal to 4. Unstable samples defined as rapidly increasing in d_h during the three measurements. * indicates only stable dispersion at an average zeta potential above −30 mV.

In the presence of low concentrations of Ca (<0.1 mM), and in the absence of any additional additive, PO_4-bearing nG (PO_4-nG) is highly unstable (Figure 4, Table 5). First, a visual assessment of the colloidal stability was made in the presence of different Ca concentrations at pH 6.0, and then on the samples which did not visually settle, d_h and zeta potential were measured. All poly-P's rendered the PO_4-nG system more stable at 0.1 mM Ca, but only PA and HMP showed a markedly more stable

DOI: 10.1021/acs.jafc.6b02425
J. Agric. Food Chem. XXXX, XXX, XXX−XXX

Table 6. Proposed Charge of Surface Complexes at pH 6.0 Based on Surface Complexation Modeling and Measured Zeta Potential of the Fe-NPs Coated with Ortho-P in the Absence or Presence of Added Polyphosphates (Phytic Acid, PA; Hexametaphosphate, HMP; and Pyrophosphate, PP), Dosed at Equal Total P Basis (Column 7) or at Equal Moles of the Polyphosphate (Column 8) in Excess of Surface Capacity

	Chemical structure at pH 6	Charge in solution per unit PO_4 at pH 6.0	Interatomic Distance(s) O-O in molecule[a] Å	Interatomic Distance(s) O-O on goethite surface[b] Å	Number of deprotonated sites per adsorbed molecule	Measured zeta potential On equal mol P base[c] mV	Measured zeta potential On equal mol base[d] mV
Ortho-P		-1.10[e]	2.35	2.57[f]-3.00[b]	0.42[g]	-34.5	-30.9
PP	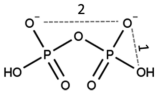	-1.11[e]	2.32-2.36 (1) 3.10-4.43 (2)	2.57[f]-3.00[b]	1[h]	-33.4	-35.2
PA	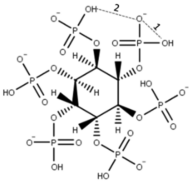	-1.12[i]	2.34-2.35 (1) 3.5-4.0 (2)	2.57[f]-3.00[b] *	2[h]	-38.2	-36.6
HMP	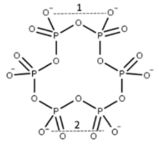	-1.00[i]	3.04-3.40 (1) 4.00-4.57 (2)	2.57[f]-3.00[b]	5[h]	-37.2	-51.0

[a]Calculated with Mercury. [b]Calculated from distance between singly coordinated oxygen atoms (oxo) at {101} goethite surface (*Pnma*) with Mercury. [c]Zeta potential at a concentration of 200 mg nG/L at 0.1 mM P as KH_2PO_4, PP, PA, or HMP at pH 6 in 1 mM NaCl. [d]Zeta potential at a concentration of 200 mg nG/L at equal dose of 1 mM P as KH_2PO_4 without or with 0.1 mM PP, PA, or HMP at pH 6.0 in 0.1 mM $CaCl_2$. [e]Calculated with JChem. [f]Measured values at bidentate binding of HPO_4^{2-}.[49] [g]Modeled with Visual Minteq at pH 6.0 with 0.1 mM PO_4^{3-} and 0.275 g goethite L^{-1} with goethite model and goethite_tpm database.[43] [h]for PP, assumption of bidentate binding of one P; for PA, 4 monodentate P bound per molecule; for HMP, 1 monodentate P bound per molecule; [i]Calculated from pK_a values.[50] *Specific adsorption mechanism for phytate involves bridging between oxo and μ-oxo layers at surface.[45]

system at 0.2 and 0.3 mM Ca (Figure 4). All poly-P treatments effects on colloidal stability could be explained by changes in the zeta potential; i.e., aggregation of poly-P-stabilized systems coincided with measured zeta potentials around −30 mV, the theoretical limit for electrostatically stabilized systems.[7] However, aggregation of the NOM stabilized system did not completely correspond with the approach to −30 mV zeta potential (Figure 4, *), which could indicate steric stabilization.

DISCUSSION

Iron Oxyhydroxide Colloids Formed by Fe(II) Oxidation. Several studies have investigated the effect of the molar PO_4:Fe ratio present during oxidation on the structure and composition of the formed particles. We therefore chose one PO_4:Fe:NOM ratio for this study and a total particle concentration slightly higher than naturally occurring to allow for zeta potential measurements. Voegelin et al.[11] conducted similar Fe(II) oxidation experiments at a comparable PO_4:Fe ratio (0.12). They reported precipitate PO_4:Fe ratio almost identical to initial dissolved PO_4:Fe ratio, this was attributed to incorporation of PO_4 in the Fe(III) precipitates. EXAFS spectra of these precipitates showed that initially Fe(III)-phosphate was formed, over time this transformed into HFO-P (60%), with a minority of lepidocrocite (37%) and goethite (5%). Other studies confirmed the formation of HFO-P up to a PO_4:Fe ratio of 0.5.[10,34−36] In our XRD patterns, no other mineral, like lepidocrocite or goethite, could be identified besides HFO-P. The presence of NOM in the current study was expected to affect the particulate PO_4:Fe molar ratio of the finally formed iron oxyhydroxides since both NOM and PO_4 are negatively charged and known to have a high affinity for iron oxyhydroxide surfaces.[21] This speculation is confirmed by stoichiometric calculations: at a specific surface area of 600 m^2/g (a conservative high estimate), the maximal surface site concentration is 0.3 mmol/L (0.9 mM Fe corresponds to 120 mg HFO/L), while 100 mg NOM/L corresponds to 0.56 mmol negative charge/L (IHSS) which might compete with 0.1 mM PO_4 present. However, this showed not to be the case (Table 2), although a higher concentration of dissolved PO_4 (7 μM PO_4) was measured compared to previous studies.[11,15] Strong sequestration of PO_4 can thus be expected in (aquatic) systems, where Fe(II) oxidizes in the presence of NOM, even when NOM is in excess. Moreover, a recent study found that Fe(II) oxidation at high DOC concentrations and low salinity led to the formation of Fe hydroxyphosphate that was colloidally stable, which was confirmed by our results.[37]

The initial molar Si:Fe ratio (0.5) was not maintained during mixed Si-Fe particle formation in the current study, and only 34% of Si was incorporated in the colloids. Previous work on iron oxidation in the presence of dissolved silica, mentions an increase in PO_4 sorption when Si is present during Fe(II) oxidation at a total Si:Fe ratio above 0.36. However, we did not find significantly reduced free P, indicating that Si has no extra PO_4 sequestering effect in the presence of NOM. Dissolved silica has already been shown to affect mineralogy in previous studies.[11,12,15] Senn et al.[12] reported that the presence of Si, at an

DOI: 10.1021/acs.jafc.6b02425
J. Agric. Food Chem. XXXX, XXX, XXX−XXX

initial PO_4:Fe < 0.5, inhibited transformation of Fe(III)-phosphate colloids into PO_4-rich ferrihydrite; instead, a Si-rich ferrihydrite layer was formed around them. According to previous studies, both NOM and Si slow down phase transformation, leading to decreasing sharpness in XRD diffractograms, which we found in the presence of Si (Figure 1).[9,34,38] In our study, however, Si did not have any additional effect in the presence of NOM on PO_4 sequestration or colloidal stability.

At the conditions of the particle formation, i.e., pH 7.0 and 50 mM Na, PO_4-Fe-NPs were kinetically stable at a zeta potential of −35 mV. When the absolute value of zeta potential of an electrostatically stabilized systems is above 30 mV, the dispersion is considered kinetically stable.[7] At a pH below 5.0 and a Ca concentration above 0.1 mM, particles started to aggregate which coincided with a zeta potential above −30 mV. This would indicate that these NOM-Fe(-Si) hydroxyphosphates are, at least partially, electrostatically stabilized. The low Ca concentration required to destabilize the system was equivalent to 0.3 mM ionic strength, well below the 50 mM ionic strength of $NaHCO_3$ under which the dispersion was stable. According to the Schulze−Hardy rule, the critical coagulation concentration (CCC) is highly dependent on the valence of the ion. The CCC is proportional to the inverse of the charge to the power six, meaning an equivalent monovalent concentration of around 7.0 mM Na for 0.1 mM Ca. This suggests a more specific effect of Ca; i.e., Ca not only compresses the EDL, leading to a decrease in surface potential and repulsion, but also is capable of cation bridging with NOM.[21] In the environment, Ca concentrations above 1.0 mM are ubiquitous in the small streams where Fe colloids are formed, and under these conditions Fe colloids are still observed. In a recent paper, colloids of different Belgian stream waters were analyzed with asymmetric flow field flow fractionation (AF4) for their composition related to size. In soft waters, they found small Fe colloids (<50 nm) with a high C:Fe molar ratio of approximately 30.[39] This high C:Fe molar ratio might explain their colloidal stability at corresponding Ca concentration to our experiments.

With this experimental setup we aimed to increase the insight in the colloidal stability of naturally formed PO_4-Fe-NPs. Our data show that Ca, and possibly other polyvalent cations like Mg and Al, control the colloidal stability of this type of particles, only in waters with a pH below 5, pH is also an important factor. Since PO_4 transport in environmental systems, similar to the experimental conditions, does occur by colloidal transport with Fe-NPs, we speculate that either fluctuations in Ca concentration or a high C:Fe ratio initially present increase colloidal stability and control PO_4 transport.

Engineered Iron Oxyhydroxide NPs. The PO_4 addition to nG shifted the IEP from 8.7 to below pH 4 for the PO_4:nG ratios in our experiments. These IEP values agree with previously published results at a comparable PO_4:nG ratio; around pH 4 for PO_4:nG = 0.45 and below pH 3 for PO_4:nG = 4.5.[40] This dramatic shift in IEP can be attributed to inner-sphere complex formation of PO_4 with nG, which is characteristic for phosphate adsorption to goethite. Phosphate anions can bind both monodentate and bidentate on goethite surfaces, with a monodentate binding resulting in a more negative resultant charge on the surface than a bidentate complex. The fraction of inner-sphere bidentate phosphate−goethite complexes increases with decreasing pH.[41] Below pH 6, more than half of the bidentate complexes are protonated, which Antelo et al.[40] found to correspond well with their electrophoresis and adsorption data. This suggested binding mechanism is compared with the surface structure of goethite (*Pnma*, {101} plane[42]). The interatomic O−O distances of PO_4 match well with those on the goethite surface, and the resultant number of deprotonated sites per phosphate molecule is modeled with Visual Minteq using the goethite surface complexation model (Table 6).[43]

The effect of additives (poly-P and NOM) showed the same trend as phosphate but yielded a comparatively larger decrease in IEP at a lower concentration. This could be related to the binding type on the goethite surface. A poly-P molecule can bind mono- or bidentate, but the resultant surface charge will be more negative compared to monophosphate because of the extra phosphate molecule(s), since per adsorbed molecule more oxygen atoms will be deprotonated (see Table 6). Theoretical interatomic O−O distances in the poly-P molecules were also compared with those on the goethite surface, to assess the possibility of bidentate binding. Comparison of these distances suggests that PO_4, pyrophosphate, and phytic acid might be able to bind bidentate because at least one interactomic O−O distance is comparable to the one on the goethite surface. The interatomic O−O distances in HMP are too large to match the O−O distance on the goethite surface, which suggests this molecule is likely to only bind monodentate, leading to more net negative charge at the surface. Phytic acid, the only investigated organic phosphate, is known to exhibit a very strong sorption in soils and on soil minerals, e.g., goethite, with K values (Langmuir coefficient, L/mol) higher than those for phosphate.[44] Adsorption of phytate on goethite is assumed to occur through four of the six phosphate groups at pH 4.5, yielding a very stable complex, a high net negative charge, and low desorption (Table 6).[45−47]

Comparison of the number of deprotonated sites, which was calculated using the probable binding mechanism, and the zeta potential measured under both equal mol and equal P mol base of PO_4, PP, PA, and HMP revealed that this explained the trend in measured zeta potential: a lower amount of deprotonated sites per adsorbed molecule corresponds with a less negative zeta potential. This trend is more pronounced on an equal mole base compared to equal P mole base. This is attributed to an incomplete coverage at the same mole P concentration for the different molecules, since only one HMP molecule can bind on the same mole P base compared to six PO_4 molecules.

For NOM, less is known about the specific binding on goethite because of a high heterogeneity in functional groups, but the strong decrease in IEP and overall charge reversal indicate inner-sphere complex formation through ligand exchange.[21,46] Increasing PO_4 concentrations had no marked additional effect on the zeta potential of NOM-coated Fe-NPs in an environmentally relevant pH range. This suggests that NOM binds stronger compared to PO_4, which is also confirmed by another study where FA showed to be a strong competitor of PO_4, which was attributed to mainly electrostatic interactions.[43] A strong increase in dispersion stability and a decrease in zeta potential at low pH were observed upon increasing the NOM concentration 5-fold (SI, Figure S6). Wang et al.[48] investigated the adsorption of FA on goethite and found that adsorption decreased with increasing pH because of competition between NOM and hydroxyls for adsorption to the goethite surface. This might explain the larger difference in zeta potential at low pH for different NOM concentrations. At a lower pH, more sites will be available for NOM sorption than at a higher pH leading to increased NOM adsorption at higher NOM concentration at low pH, lowering the zeta potential and, consequently, increasing the

DOI: 10.1021/acs.jafc.6b02425
J. Agric. Food Chem. XXXX, XXX, XXX−XXX

stability. However, Ca addition rapidly reduced the zeta potential, leading to unstable dispersions. Ca, as a divalent electrolyte, can not only compress the EDL but also form complexes with NOM, leading to a partial neutralization of negative charge and a change in NOM conformation, thereby also affecting steric stabilization.[21] Since destabilization did not fully correspond with a zeta potential above −30 mV, some steric stabilization appears to be present in this setup.

To summarize, we have identified NOM and poly-P's, specifically PA and HMP, as potentially good candidates to stabilize PO_4-nG over a wide pH range with zeta potential measurements pointing to systems which are predominantly stabilized through electrostatic repulsion. Hydrodynamic diameters of the stabilized PO_4-nG were larger than those of the uncoated nG; however, the diameter measured with spICP-MS was almost identical, indicating that the stabilizers have a large influence on the thickness of the EDL. Chemical modeling and surface binding mechanisms for the different poly-P's explain the trends in zeta potential measurements; i.e., the poly-P's bind with less than all PO_4 moieties to the surface, rendering more negative charge to the surface compared to orthophosphate anions only. However, in-depth experimental studies are required to confirm these suggested binding mechanisms. PO_4-nG dispersions were unstable at very low Ca concentrations (0.1 mM), but HMP-stabilized PO_4-nG dispersions remained kinetically stable up to 0.3 mM $CaCl_2$. These findings show that P nanofertilizers, as HMP-stabilized PO_4-nG, might be a more efficient alternative to traditional fertilizers in P-depleted soils with low Ca. Because these NPs can remain mobile in solution and migrate to the plant rhizosphere, PO_4 can desorb locally to meet plant demands with reduced loss by sorption on soil minerals.

■ ASSOCIATED CONTENT

Supporting Information

The Supporting Information is available free of charge on the ACS Publications website at DOI: 10.1021/acs.jafc.6b02425.

Preliminary tests for increasing nG colloidal stability with additives (Table S1); additional characterization of nG (Section 2); surface complexation reactions for modeling (Section 3); hydrodynamic diameter of iron oxyhydroxide fractions formed by Fe(II) oxidation (Table S7); zeta potential measurements for nG (Figures S5 and S6) (PDF)

■ AUTHOR INFORMATION

Corresponding Author

*E-mail: jessica.bollyn@kuleuven.be. Phone: +32 16 37 20 44.

Present Address

#S.B.: European Copper Institute, Avenue de Tervueren 168 b-10, 1150 Brussels, Belgium

Funding

J.B. thanks the FWO-Research Foundation Flanders for a PhD fellowship.

Notes

The authors declare no competing financial interest.

■ ACKNOWLEDGMENTS

Thanks to Kristin Coorevits and Karlien Cassaert for assistance, Dr. Ivo Stassen (Dept. of Microbial and Molecular Systems) for BET analysis, Maarten Everaert and Kris Dox (Dept. of Earth and Environmental Sciences) for help with the XRD analysis, Ruud Peeters (RIKILT, Wageningen) for the spICP-MS calculation sheet, and Dr. Andreas Fritzsche (Friedrich-Schiller University Jena) for the SEM measurements. We thank the three anonymous reviewers for comments that improved the quality of the paper.

■ ABBREVIATIONS USED

Fe-NPs, iron oxyhydroxide nanoparticles; FA, fulvates; PA, phytic acid; HMP, hexametaphosphate; NOM, natural organic matter; PO_4-Fe-NPs, phosphate-coated iron oxyhydroxide nanoparticles; HFO, hydrous ferric oxide; d_h, Z-average hydrodynamic diameter; nG, nano-goethite; TPP, tripolyphosphate; PP, pyrophosphate; TMP, trimetaphosphate; poly-P, polyphosphate

■ REFERENCES

(1) Frossard, E.; Brossard, M.; Hedley, M. J.; Metherell, A. Reactions Controlling the Cycling of P in Soils. *Phosphorus in the global environment. Transfers, cycles and management*, SCOPE 54; Wiley: New York, 1995; pp 107−138.

(2) Montalvo, D.; Degryse, F.; McLaughlin, M. J. Natural colloidal P and its contribution to plant P uptake. *Environ. Sci. Technol.* **2015**, *49*, 8267−8267.

(3) Hens, M.; Merckx, R. The role of colloidal particles in the speciation and analysis of "dissolved" phosphorus. *Water Res.* **2002**, *36*, 1483−1492.

(4) Regelink, I. C.; Voegelin, A.; Weng, L.; Koopmans, G. F.; Comans, R. N. J. Characterization of Colloidal Fe from Soils Using Field-Flow Fractionation and Fe K-Edge X-ray Absorption Spectroscopy. *Environ. Sci. Technol.* **2014**, *48*, 4307−4316.

(5) Waychunas, G. A.; Kim, C. S.; Banfield, J. F. Nanoparticulate iron oxide minerals in soils and sediments: Unique properties and contaminant scavenging mechanisms. *J. Nanopart. Res.* **2005**, *7*, 409−433.

(6) Tipping, E. The adsorption of aquatic humic substances by iron oxides. *Geochim. Cosmochim. Acta* **1981**, *45*, 191−199.

(7) Hiemenz, P. C.; Rajagopalan, R. *Principles of Colloid and Surface Chemistry*, 3rd ed.; Marcel Dekker, Inc.: New York, 1997.

(8) Degryse, F.; Smolders, E.; Parker, D. R. Partitioning of metals (Cd, Co, Cu, Ni, Pb, Zn) in soils: concepts, methodologies, prediction and applications - a review. *Eur. J. Soil Sci.* **2009**, *60*, 590−612.

(9) Mayer, T. D.; Jarrell, W. M. Phosphorus sorption during iron(II) oxidation in the presence of dissolved silica. *Water Res.* **2000**, *34*, 3949−3956.

(10) Gunnars, A.; Blomqvist, S.; Johansson, P.; Andersson, C. Formation of Fe(III) oxyhydroxide colloids in freshwater and brackish seawater, with incorporation of phosphate and calcium. *Geochim. Cosmochim. Acta* **2002**, *66*, 745−758.

(11) Voegelin, A.; Senn, A. C.; Kaegi, R.; Hug, S. J.; Mangold, S. Dynamic Fe-precipitate formation induced by Fe(II) oxidation in aerated phosphate-containing water. *Geochim. Cosmochim. Acta* **2013**, *117*, 216−231.

(12) Senn, A.; Kaegi, R.; Hug, S. J.; Hering, J. G.; Mangold, S.; Voegelin, A. Composition and structure of Fe (III) -precipitates formed by Fe (II) oxidation in water at near-neutral pH: Interdependent effects of phosphate, silicate and Ca. *Geochim. Cosmochim. Acta* **2015**, *162*, 220−246.

(13) Cornelis, G.; Hund-Rinke, K.; Kuhlbusch, T.; Van den Brink, N.; Nickel, C. Fate and bioavailability of engineered nanoparticles in soils: a review. *Crit. Rev. Environ. Sci. Technol.* **2014**, *44*, 2720−2764.

(14) Baken, S.; Sjöstedt, C.; Gustafsson, J. P.; Seuntjens, P.; Desmet, N.; De Schutter, J.; Smolders, E. Smolders, E. Characterisation of hydrous ferric oxides derived from iron-rich groundwaters and their contribution to the suspended sediment of streams. *Appl. Geochem.* **2013**, *39*, 59−68.

(15) Voegelin, A.; Kaegi, R.; Frommer, J.; Vantelon, D.; Hug, S. J. Effect of phosphate, silicate, and Ca on Fe(III)-precipitates formed in

DOI: 10.1021/acs.jafc.6b02425
J. Agric. Food Chem. XXXX, XXX, XXX−XXX

aerated Fe(II)- and As(III)-containing water studied by X-ray absorption spectroscopy. *Geochim. Cosmochim. Acta* **2010**, *74*, 164−186.
(16) Angelico, R.; Ceglie, A.; He, J. Z.; Liu, Y. R.; Palumbo, G.; Colombo, C. Particle size, charge and colloidal stability of humic acids coprecipitated with ferrihydrite. *Chemosphere* **2014**, *99*, 239−247.
(17) Châtellier, X.; West, M. M.; Rose, J.; Fortin, D.; Leppard, G. G.; Ferris, F. G. Characterization of Iron-Oxides Formed by Oxidation of Ferrous Ions in the Presence of Various Bacterial Species and Inorganic Ligands. *Geomicrobiol. J.* **2004**, *21*, 99−112.
(18) Zhang, Y.; Chen, Y.; Westerhoff, P.; Crittenden, J. Impact of natural organic matter and divalent cations on the stability of aqueous nanoparticles. *Water Res.* **2009**, *43*, 4249−4257.
(19) Sander, S.; Mosley, L. M.; Hunter, K. A. Investigation of interparticle forces in natural waters: Effects of adsorbed humic acids on iron oxide and alumina surface properties. *Environ. Sci. Technol.* **2004**, *38*, 4791−4796.
(20) Chekli, L.; Phuntsho, S.; Roy, M.; Shon, H. K. Characterisation of Fe-oxide nanoparticles coated with humic acid and Suwannee River natural organic matter. *Sci. Total Environ.* **2013**, *461*−*462*, 19−27.
(21) Philippe, A.; Schaumann, G. E. Interactions of dissolved organic matter with natural and engineered inorganic colloids: a review. *Environ. Sci. Technol.* **2014**, *48*, 8946−8962.
(22) Christian, P.; Von Der Kammer, F.; Baalousha, M.; Hofmann, T. Nanoparticles: Structure, properties, preparation and behaviour in environmental media. *Ecotoxicology* **2008**, *17*, 326−343.
(23) Cornelis, G. Fate descriptors for engineered nanoparticles: the good, the bad, and the ugly. *Environ. Sci.: Nano* **2015**, *2*, 19−26.
(24) Gogos, A.; Knauer, K.; Bucheli, T. D. Nanomaterials in plant protection and fertilization: Current state, foreseen applications, and research priorities. *J. Agric. Food Chem.* **2012**, *60*, 9781−9792.
(25) Zhang, W.-X. Nanoscale iron particles for enviornmental remediation: An overview. *J. Nanopart. Res.* **2003**, *5*, 323−332.
(26) Zahra, Z.; Arshad, M.; Rafique, R.; Mahmood, A.; Habib, A.; Qazi, I. a; Khan, S. a. Metallic Nanoparticles (TiO2 and Fe3O4) Application Modify Rhizosphere Phosphorus Availability and Uptake by Lactuca sativa. *J. Agric. Food Chem.* **2015**, *63*, 6876−6882.
(27) Bansiwal, A. K.; Rayalu, S. S.; Labhasetwar, N. K.; Juwarkar, A. A.; Devotta, S. Surfactant-modified zeolite as a slow release fertilizer for phosphorus. *J. Agric. Food Chem.* **2006**, *54*, 4773−4779.
(28) Davidson, D.; Gu, F. X. Materials for sustained and controlled release of nutrients and molecules to support plant growth. *J. Agric. Food Chem.* **2012**, *60*, 870−876.
(29) Erro, J.; Urrutia, O.; San Francisco, S.; Garcia-Mina, J. M. Development and agronomical validation of new fertilizer compositions of high bioavailability and reduced potential nutrient losses. *J. Agric. Food Chem.* **2007**, *55*, 7831−7839.
(30) Baken, S.; Verbeeck, M.; Verheyen, D.; Diels, J.; Smolders, E. Phosphorus losses from agricultural land to natural waters are reduced by immobilization in iron-rich sediments of drainage ditches. *Water Res.* **2015**, *71*, 160−170.
(31) Lee, S.; Bi, X.; Reed, R. B.; Ranville, J. F.; Herckes, P.; Westerhoff, P. Nanoparticle size detection limits by single particle ICP-MS for 40 elements. *Environ. Sci. Technol.* **2014**, *48*, 10291−10300.
(32) Thibault, P. J.; Rancourt, D. G.; Evans, R. J.; Dutrizac, J. E. Mineralogical confirmation of a near-P:Fe = 1:2 limiting stoichiometric ratio in colloidal P-bearing ferrihydrite-like hydrous ferric oxide. *Geochim. Cosmochim. Acta* **2009**, *73*, 364−376.
(33) Kosmulski, M. pH-dependent surface charging and points of zero charge. IV. Update and new approach. *J. Colloid Interface Sci.* **2009**, *337*, 439−448.
(34) van der Grift, B.; Rozemeijer, J. C.; Griffioen, J.; van der Velde, Y. Iron oxidation kinetics and phosphate immobilization along the flow-path from groundwater into surface water. *Hydrol. Earth Syst. Sci.* **2014**, *18*, 4687−4702.
(35) Baken, S.; Moens, C.; van der Grift, B.; Smolders, E. Phosphate binding by natural iron-rich colloids in streams. *Water Res.* **2016**, *98*, 326−333.
(36) Sahai, N.; Lee, Y. J.; Xu, H.; Ciardelli, M.; Gaillard, J. F. Role of Fe(II) and phosphate in arsenic uptake by coprecipitation. *Geochim. Cosmochim. Acta* **2007**, *71*, 3193−3210.
(37) van der Grift, B.; Behrends, T.; Osté, L. A.; Schot, P. P.; Wassen, M. J.; Griffioen, J. Fe hydroxyphosphate precipitation and Fe (II) oxidation kinetics upon aeration of Fe (II) and phosphate-containing synthetic and natural solutions. *Geochim. Cosmochim. Acta* **2016**, *186*, 71−90.
(38) Gerke, J. Phosphate adsorption by humic/Fe-oxide mixtures aged at pH 4 and 7 and by poorly ordered Fe-oxide. *Geoderma* **1993**, *59*, 279−288.
(39) Baken, S.; Regelink, I. C.; Comans, R. N. J.; Smolders, E.; Koopmans, G. F. Iron-rich colloids as carriers of phosphorus in streams: A field- flow fractionation study. *Water Res.* **2016**, *99*, 83−90.
(40) Antelo, J.; Avena, M.; Fiol, S.; López, R.; Arce, F. Effects of pH and ionic strength on the adsorption of phosphate and arsenate at the goethite−water interface. *J. Colloid Interface Sci.* **2005**, *285*, 476−486.
(41) Hiemstra, T.; Van Riemsdijk, W. H. A Surface Structural Approach to Ion Adsorption: The Charge Distribution (CD) Model. *J. Colloid Interface Sci.* **1996**, *179*, 488−508.
(42) Schwertmann, U.; Cornell, R. M. *Iron Oxides in the Laboratory. Preparation and Characterization*, 2nd ed.; Wiley-VCH: Weinheim, 2000.
(43) Weng, L.; van Riemsdijk, W. H.; Hiemstra, T. Humic nanoparticles at the oxide-water interface: Interactions with phosphate ion adsorption. *Environ. Sci. Technol.* **2008**, *42*, 8747−8752.
(44) Turner, B. L.; Frossard, E.; Baldwin, D. S. *Organic Phosphorus in the Environment*; CABI Publishing, Oxfordshire, UK, 2005.
(45) Celi, L.; Presta, M.; Ajmore-Marsan, F.; Barberis, E. Effects of pH and Electrolytes on Inositol Hexaphosphate Interaction with Goethite. *Soil Sci. Soc. Am. J.* **2001**, *65*, 753−760.
(46) Ruyter-Hooley, M.; Morton, D. W.; Johnson, B. B.; Angove, M. J. The effect of humic acid on the sorption and desorption of myo-inositol hexaphosphate to gibbsite and kaolinite. *Eur. J. Soil Sci.* **2016**, *67*, 285−293.
(47) Martin, M.; Celi, L.; Barberis, E. Desorption and Plant Availability of Myo-Inositol Hexaphosphate Adsorbed on Goethite. *Soil Sci.* **2004**, *169*, 115−124.
(48) Wang, L.; Chin, Y.-P.; Traina, S. J. Adsorption of (poly)maleic acid and an aquatic fulvic acid by goethite. *Geochim. Cosmochim. Acta* **1997**, *61*, 5313−5324.
(49) Paul, K. W. Molecular Modeling Study of Sulfate and Phosphate Adsorption at the Mineral-Water Interface. Ph.D. thesis, University of Delaware, 2007.
(50) Costello, A. J. R.; Glonek, T.; Myers, T. C. 31P nuclear magnetic resonance-pH titrations of myo-inositol hexaphosphate. *Carbohydr. Res.* **1976**, *46*, 159−171.

DOI: 10.1021/acs.jafc.6b02425
J. Agric. Food Chem. XXXX, XXX, XXX−XXX